AJVR

Candidate urinary biomarkers show promise for distinguishing between calcium oxalate versus struvite urolithiasis in dogs

Chu Xu, MS[1,2]; Yufei Yang, BS[1,2]; Zhurui Shao, BS[1,2]; Ruizi Ren, BS[1,2]; Yiwen Zhang, BS[1,2]; Yipeng Jin, PhD[1,2*]; Hao Shi, DVM[1,2*]

[1]The Clinical Department, College of Veterinary Medicine, China Agricultural University, Beijing, China
[2]China Agricultural University Veterinary Teaching Hospital, Beijing, China

*Corresponding author: Dr. Jin (yipengjin@cau.edu.cn); Dr. Shi (haoshi@cau.edu.cn)

OBJECTIVE
To identify metabolites and metabolic pathways affected in dogs with struvite and calcium oxalate urolithiasis compared to healthy dogs. To explore the candidate urinary biomarkers to distinguish dogs with struvite and calcium oxalate urolithiasis.

ANIMALS
13 dogs with calcium oxalate urolithiasis, 7 dogs with struvite urolithiasis, and 13 healthy dogs were recruited between September 2021 and January 2023.

METHODS
Metabolomic profiles were analyzed from urine samples using UPLC-MS MS. According to the variable importance in the projection (> 1) and correlation coefficient ($P < .05$) obtained by orthogonal partial least squares discriminant analysis, the differential metabolites were screened. The Kyoto Encyclopedia of Genes and Genomes database was used to identify the metabolic pathways involved.

RESULTS
Compared to healthy dogs, those with calcium oxalate urolithiasis exhibited distinct metabolites primarily associated with phenylalanine metabolism, nicotinic acid, and nicotinamide metabolic pathways. Conversely, dogs with struvite urolithiasis demonstrated variations in metabolites mainly linked to tryptophan metabolism and glycerophospholipid metabolic pathways. Between calcium oxalate and struvite groups, pyocyanin, glycylprolylarginine, traumatin, cysteinyl-leucine, and 8-hydroxydodecylcarnitine are candidate urinary biomarkers.

CLINICAL RELEVANCE
Our findings provide an in-depth analysis of metabolic perturbations associated with calcium oxalate and struvite urolithiasis in dogs. We also identified candidate urinary biomarkers distinguishing between dogs with calcium oxalate and struvite urolithiasis, which can be subsequently validated to assist in stone diagnosis and guide treatment choices.

Keywords: urolithiasis, dogs, urinary metabolomics, differential metabolites, biomarker

Urolithiasis is a common clinical urological disorder in dogs and can be classified as urethral calculus, cystourolith, and nephrolithiasis. Urinary calculi can irritate the mucosa of the urinary tract, causing bleeding, inflammation, and obstruction in the urinary tract of affected dogs, which can seriously affect their quality of life.[1] The pathogenesis of canine urolithiasis is still unclear, and the causes of the disease are generally considered to be broad, such as dietary habits, body mineral metabolism disorder, abnormal urinary pH, and urinary tract infections (UTIs).[2,3] Metabolomics is a method to study the intermediate and final products of physiological metabolism. With the help of bioinformatics, it is possible to explore extremely large collections of compounds, free from the constraints of traditional biochemical research methods.[4] Urine metabolomics analysis has helped in exploring the mechanism of disease and diagnosing urological diseases such as cystitis and UTIs.[5–7] Interstitial cystitis/painful bladder syndrome is a chronic syndrome of unknown etiology that presents with bladder pain, urinary frequency, and urgency. The lack of specific biomarkers and a

Received September 25, 2023
Accepted January 3, 2024

doi.org/10.2460/ajvr.23.09.0214

poor understanding of underlying molecular mechanisms present challenges for disease diagnosis and therapy. Relevant research has identified noninvasive biomarker candidates for cystitis from urine specimens and potentially gained new insight into disease mechanisms. Human medical research was the first to carry out a series of urine metabolomics studies on urolithiasis and found that urolithiasis patients had characteristic urine metabolites.[8] Calcium oxalate and struvite stones are the most common types of stones in clinical cases of canine urolithiasis, and the treatment approaches for these 2 types of stones are different. Calcium oxalate stones require surgical removal, whereas struvite stones can be treated through dietary dissolution therapy.[9] To our knowledge, no urinary metabolomics studies have been performed for canine urolithiasis and specific stone types. There is also a lack of clinical methods for determining types of stones before surgery.

In this study, urine metabolomics analysis was conducted on healthy control dogs, as well as dogs with calcium oxalate and struvite urolithiasis. The aim was to gain a comprehensive understanding of the metabolic changes associated with canine urolithiasis and to identify candidate urinary biomarkers that could potentially distinguish between these 2 types of stones.

Methods

Sample collection and clinical information

From September 2021 to January 2023, urine samples were collected from 13 dogs with calcium oxalate stone (CaOx group), 7 dogs with struvite stone (struvite group), and 13 healthy dogs (control group) in China Agricultural University Veterinary Teaching Hospital (Beijing, China) **(Table 1)**. Complete blood count, biochemistry, and urinalysis were performed in each case to ensure that the dog was free of other metabolic diseases such as diabetes, hypercholesterolemia, hyperlipidemia, and obesity. All of the stones were confirmed to consist of either calcium oxalate or struvite after surgery. Urinary tract infection was determined by culture of the stones and bladder mucosa, which was found only in the struvite group (5/7 dogs). All tested dogs were from the Beijing area to minimize the regional differences. Detailed information including breeds, dietary habits, and abnormal blood test results of dogs with urolithiasis is shown **(Supplementary Tables 1–3)**. All the samples were collected before any medical or surgical treatment. A 5-mL urine sample was collected from each case by cystocentesis or catheterization. The urine samples were centrifuged at 1,000 X *g* for 15 minutes and then 10,000 X *g* for 10 minutes, the mid stage clarified urine was aspirated, 1 mL of each tube was precisely measured, and the sample was frozen at −80 °C. The animal study was reviewed and approved by the College of Veterinary Medicine, China Agricultural University. Informed client consent was obtained for each dog before enrollment in the study.

Sample pretreatment

A 100-µL liquid sample was added to a 1.5-mL centrifuge tube with 400 µL solution (acetonitrile:methanol = 1:1 [vol:vol]) containing 0.02 mg/mL internal standard (L-2-chlorophenylalanine) to extract metabolites. The samples were mixed by vortex for 30 seconds and low-temperature sonicated for 30 minutes (5 °C, 40 kHz). The samples were placed at −20 °C for 30 minutes to precipitate the proteins. Then, the samples were centrifuged at 13,000 X *g* and 4 °C for 15 minutes. The supernatant was removed and blown dry under nitrogen. The sample was then resolubilized with 100 µL solution (acetonitrile:water = 1:1) and extracted by low-temperature ultrasonication for 5 minutes (5 °C, 40 kHz), followed by centrifugation at 13,000 X *g* and 4 °C for 10 minutes. The supernatant was transferred to sample vials for LC-MS-MS analysis.

Quality control sample

As a part of the system conditioning and quality control process, a pooled quality control sample (QC) was prepared by mixing equal volumes of all samples. The QC samples were disposed of and tested in the same manner as the analytic samples. This helped to represent the whole sample set, which would be injected at regular intervals (every 10 samples) to monitor the stability of the analysis.

UPLC-MS-MS

The UPLC-MS-MS analysis of the sample was conducted using a Thermo Ultra-High Performance Liquid Chromatography-Quadrupole (UHPLC-Q)

Table 1—Clinical characteristics of dogs with calcium oxalate urolithiasis (n = 13), dogs with struvite urolithiasis (7), and healthy control dogs (13).

Variables	Calcium oxalate	Struvite	Control	*P* value
Dogs enrolled (n)	13	7	13	–
Dogs with positive urine, urolith nidi, or bladder mucosal biopsy culture (n)	0	5	0	–
Age (y)[a]	9.5 (5.0–15.0)	6.4 (4.0–11.0)	6.3 (1.0–11.0)	.057
Weight (kg)[a]	9.4 (2.6–28.0)	12.2 (6.9–25.0)	14.5 (3.2–41.7)	.375
Males, intact/castrated (n)	6/3	2/0	4/2	–
Females, intact/spayed (n)	1/3	1/4	4/3	–

[a]Data are reported as median and range.
– = Not calculated.

Exactive HF-X system equipped with an ACQUITY HSS T3 column (100 × 2.1-mm inner diameter, 1.8 µm; Waters Corp) at Majorbio Bio-Pharm Technology Co Ltd. The mobile phases consisted of 0.1% formic acid in water:acetonitrile (95:5, vol/vol; solvent A) and 0.1% formic acid in acetonitrile:isopropanol:water (47.5:47.5, vol/vol; solvent B). Positive ion mode separation gradient consisted of 0 to 3 minutes, mobile phase B increased from 0% to 20%; 3 to 4.5 minutes, mobile phase B increased from 20% to 35%; 4.5 to 5 minutes, mobile phase B increased from 35% to 100%; 5 to 6.3 minutes, mobile phase B maintained at 100%; 6.3 to 6.4 minutes, mobile phase B decreased from 100% to 0%; and 6.4 to 8 minutes, mobile phase B maintained at 0%. Separation gradient in negative ion mode consisted of 0 to 1.5 minutes, mobile phase B increased from 0 to 5%; 1.5 to 2 minutes, mobile phase B increased from 5% to 10%; 2 to 4.5 minutes, mobile phase B increased from 10% to 30%; 4.5 to 5 minutes, mobile phase B increased from 30% to 100%; 5 to 6.3 minutes, mobile phase B linearly maintained 100%; 6.3 to 6.4 minutes, the mobile phase B decreased from 100% to 0%; and 6.4 to 8 minutes, the mobile phase B linearly maintained at 0%. The flow rate was 0.40 mL/min, and the column temperature was 40 °C.

MS conditions—The MS data were collected using a Thermo UHPLC-Q Exactive HF-X Mass Spectrometer equipped with an electrospray ionization (ESI) source operating in positive ion mode and negative ion mode. The optimal conditions were set as follows: source temperature was set at 425 °C; sheath gas flow rate was set at 50 arb; Aux gas flow rate was set at 13 arb; and ion-spray voltage floating was set at −3,500 V in negative ion mode and 3,500 V in positive ion mode, respectively; normalized collision energy was set at 20–40–60 V rolling for MS-MS. Full MS resolution was set at 60,000, and MS-MS resolution was set at 7,500. Data acquisition was performed with the Data Dependent Acquisition mode. The detection was carried out over a mass range of 70 to 1,050 m/z.

Data processing and analysis

After ultraperformance liquid chromatography-time of flight/mass spectrometry analyses, the raw data were imported into the Progenesis QI software[10] (version 3.0; Waters Corp) for baseline filtering, peak picking, retention time correction, and peak alignment. The preprocessing results generated a data matrix that consisted of the retention time, m/z values, and peak intensity. MS and MS-MS spectral information were matched in reliable biochemical databases such as the Human metabolome database,[11] Metlin database,[12] and Majorbio cloud platform.[13] In all samples, the ESI+ mode detected 6,446 feature peaks, and 1,427 metabolites were annotated; the ESI− mode detected 6,709 feature peaks, and 999 metabolites were annotated.

To enhance data analysis, appropriate preprocessing of raw sampling data generated by the instrument was performed to eliminate or reduce errors introduced during the experimental and analytical processes, ensuring data structure standardization. The data preprocessing procedure includes filtering, imputation, normalization, and logarithmic transformation. Initially, this involved the removal of missing values of metabolic features in the raw data matrix, and at least 80% of nonzero metabolites in any set of samples were retained. After filtering, the vacancy values were imputed with the minimum value of the raw data matrix, reducing errors from sample preparation and instrument instability. Each metabolic feature was normalized by MS "total useful signal."[14] The signal intensity of each peak detected by LC-MS was calculated by integrating the signal intensities of all peaks in each sample as the total useful signal. The relative abundance of metabolites was normalized by dividing the intensity of each peak in each sample by the sum of the intensities of all peaks in each sample (total useful signal) and multiplying it by the maximum of the sum of the intensities of all peaks in all samples, which was used as the metabolite normalized relative abundance for subsequent correlation analyses. The Python package "Scipy.stats"[15] (version 1.0.0; Pauli Virtanen, 2022) was used to perform the proprietary algorithm during the normalization. The entire data matrix underwent QC validation, calculating the relative standard deviation (RSD) of each feature peak in QC samples. Features with RSD greater than 30% were excluded, as metabolites with RSD greater than 30% are generally considered to exhibit significant fluctuations during the experimental process and are not suitable for data analysis. Following normalization, statistical analysis was performed on log-transformed data, resulting in a final data matrix comprising 1,689 retained metabolites (ESI+ mode, 967; ESI− mode, 722) for subsequent data analysis.

Then, the R package "ropls"[16] (version 1.6.2; Etienne Thevenot, 2022) was used to perform principal component analysis and orthogonal least partial squares discriminant analysis (OPLS-DA) and 7-cycle interactive validation evaluating the stability of the model. The metabolites with a variable importance in the projection (VIP) greater than 1 and a *P* value less than .05 were determined as significantly different metabolites based on the VIP obtained by the OPLS-DA model and the *P* value generated by the Student *t* test.

Differential metabolites among the 2 groups were mapped into their biochemical pathways through metabolic enrichment and pathway analysis based on Kyoto Encyclopedia of Genes and Genomes (KEGG) database.[17] These metabolites could be classified according to the pathways they are involved in or the functions they perform. Enrichment analysis was used to analyze a group of metabolites in a function node whether appears or not. The principle was that the annotation analysis of a single metabolite develops into an annotation analysis of a group of metabolites. The Python package "Scipy.stats"[15] (version 1.0.0; Pauli Virtanen, 2022) was used to perform enrichment analysis to obtain the most relevant biological pathways for experimental treatments.

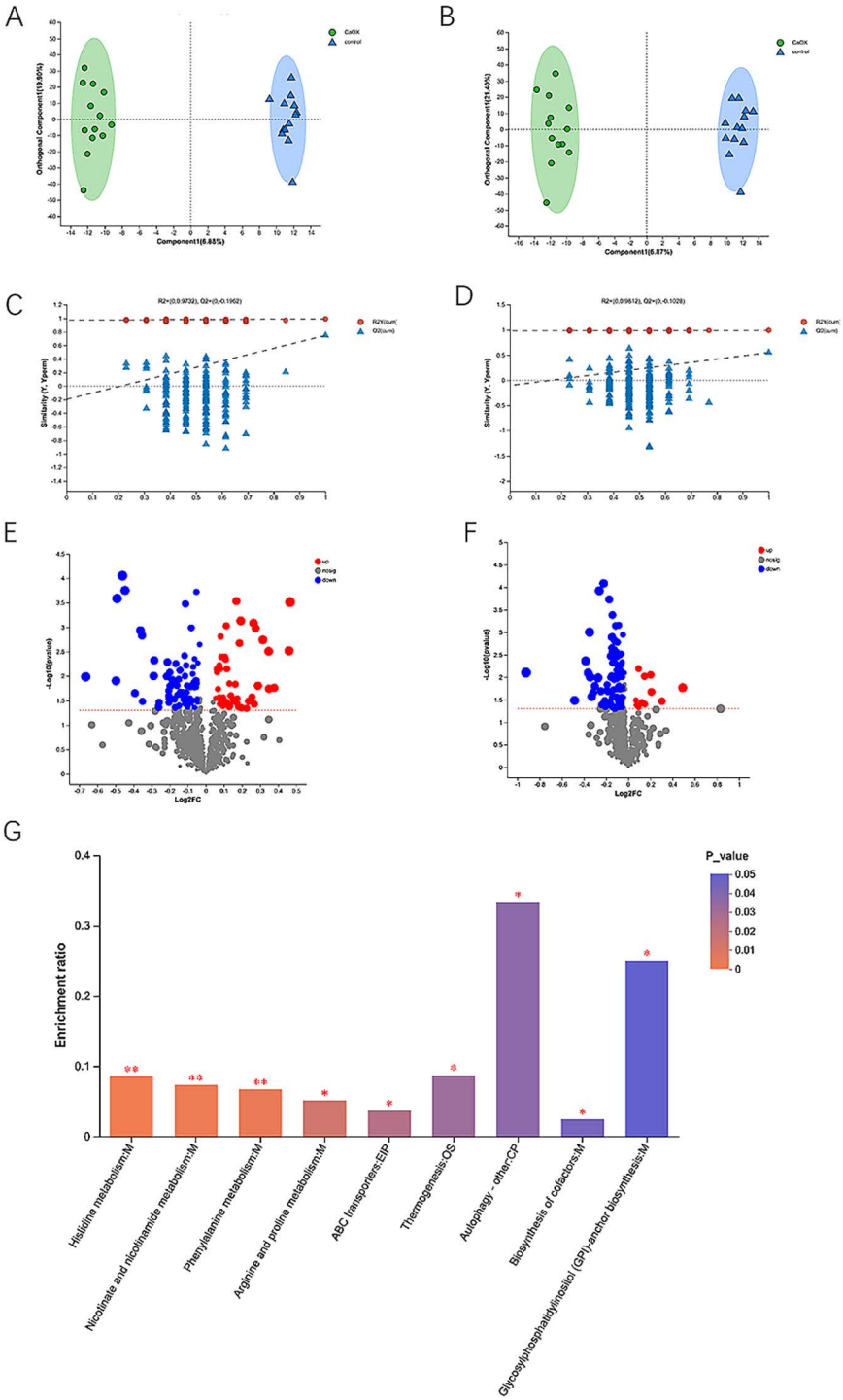

Figure 1—Urine metabolomics analysis was conducted in dogs with calcium oxalate (CaOx) urolithiasis (n = 13) and healthy control dogs (13) to explore important metabolites and related metabolic pathways in the urine of dogs with CaOx urolithiasis. The orthogonal partial least squares discriminant analysis (OPLS-DA) model under the electrospray ion source-positive (ESI+) mode (A) and electrospray ion source-negative (ESI−) mode (B): the green dots represent the CaOx group, and the blue dots represent the control group. A clear separation between the 2 groups means metabolic differences. The permutation test plot of OPLS-DA under the ESI+ mode (C) and ESI− mode (D): the red dots represent the value of R2Y, and the blue dots represent the value of Q2. R2Y was used to assess fitness, and Q2 indicated the predictive ability of the model. Volcanic map of differential metabolites in the urine of healthy dogs and dogs with CaOx urolithiasis under the ESI+ mode (E) and ESI− mode (F): according to variable importance in the projection (VIP) value > 1 and *P* value < .05, the red dots represent selected upregulated metabolites, the blue dots represent selected downregulated metabolites, and the gray dots represent filtered metabolites. Kyoto Encyclopedia of Genes and Genomes (KEGG) pathway analysis in CaOx group as compared to control group (G): the color gradient indicates the significance of enrichment. Log2FC = Log_2 fold change. CP = Cellular Processe. EIP = Environmental Information Processing. M = Metabolism. OS = Organismal Systems. **P* < .05; ***P* < .01.

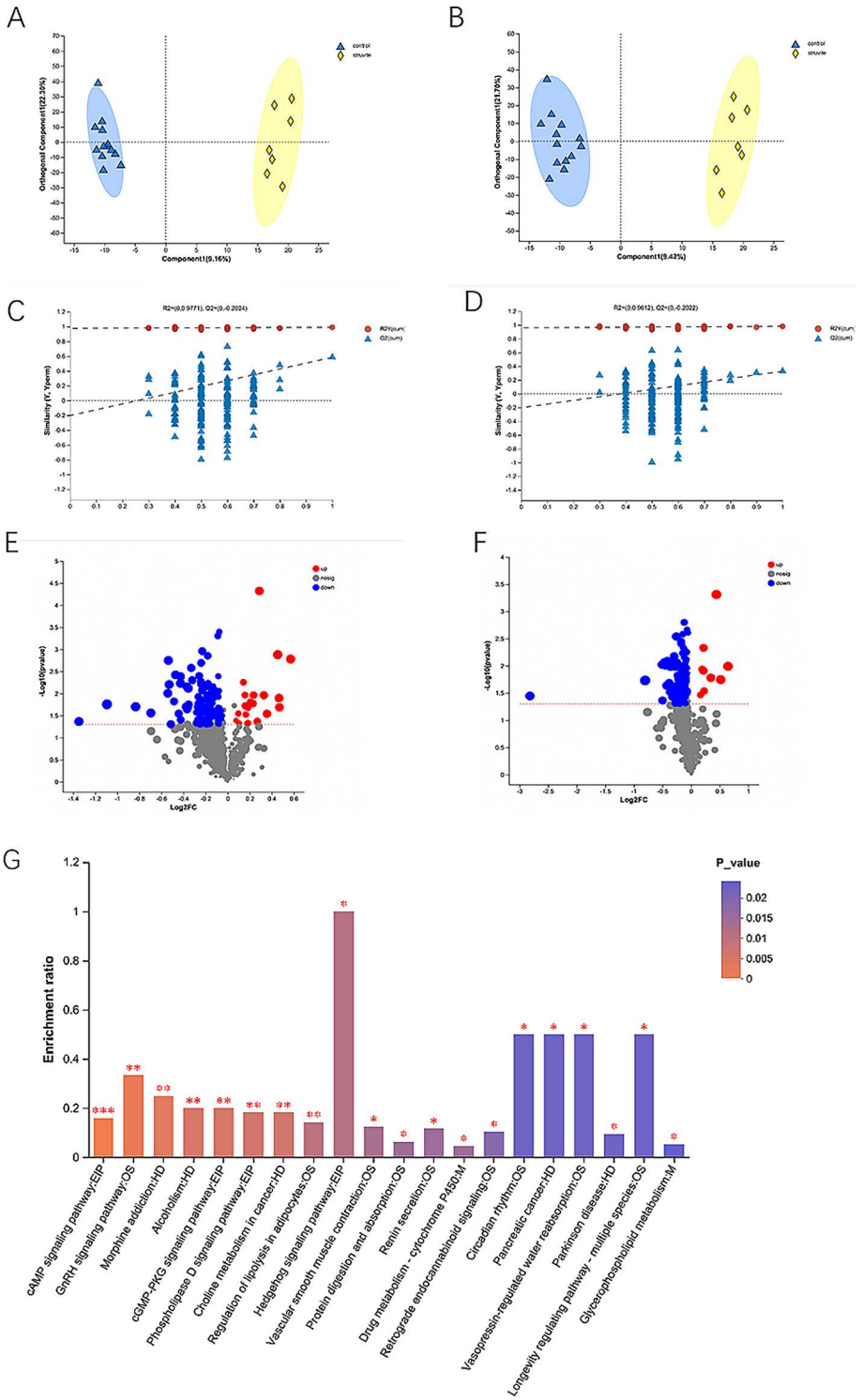

Figure 2—Urine metabolomics analysis was conducted in dogs with struvite urolithiasis (n = 7) and healthy control dogs (13) to explore important metabolites and related metabolic pathways in the urine of dogs with struvite urolithiasis. The OPLS-DA model under the ESI+ mode (A) and ESI− mode (B): the yellow dots represent the struvite group, and the blue dots represent the control group. A clear separation between the 2 groups means metabolic differences. The permutation test plot of OPLS-DA under the ESI+ mode (C) and ESI− mode (D): the red dots represent the value of R2Y, and the blue dots represent the value of Q2. R2Y was used to assess fitness, and Q2 indicated the predictive ability of the model. Volcanic map of differential metabolites in the urine of healthy dogs and dogs with struvite urolithiasis under the ESI+ ion mode (E) and ESI− ion mode (F): according to the VIP value > 1 and *P* value < .05, the red dots represent selected upregulated metabolites, the blue dots represent selected downregulated metabolites, the gray dots represent filtered metabolites. KEGG pathway analysis in struvite group as compared to control group (G): the color gradient indicates the significance of enrichment. HD = Human Diseases. **P* < .05, ***P* < .01, and ****P* < .001.

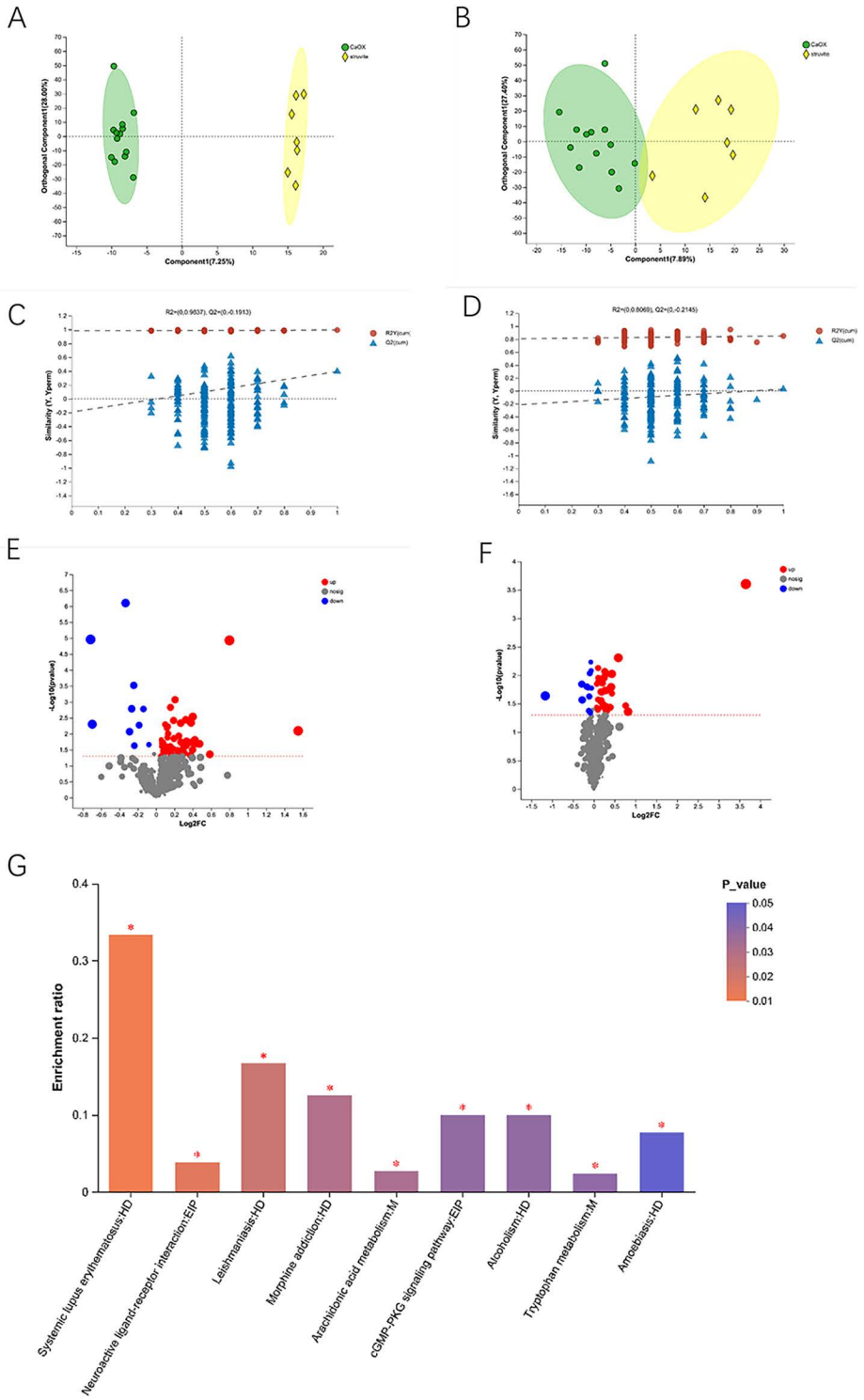

Figure 3—Urine metabolomics analysis was conducted in dogs with CaOx urolithiasis (n = 13) and dogs with struvite urolithiasis (7) to explore important metabolites and related metabolic pathways between the urine of dogs with CaOx and struvite urolithiasis. The OPLS-DA model under the ESI+ mode (A) and ESI− mode (B): the green dots represent the CaOx group, and the yellow dots represent the struvite group. A clear separation between the 2 groups means metabolic differences. The permutation test plot of OPLS-DA under the ESI+ mode (C) and ESI− mode (D): the red dots represent the value of R2Y, and the blue dots represent the value of Q2. R2Y was used to assess fitness, and Q2 indicated the predictive ability of the model. Volcanic map of differential metabolites in the urine of dogs with CaOx urolithiasis and dogs with struvite urolithiasis under the ESI+ mode (E) and ESI− mode (F): according to VIP value > 1 and *P* value < .05, the red dots represent selected upregulated metabolites, the blue dots represent selected downregulated metabolites, and the gray dots represent filtered metabolites. KEGG pathway analysis in CaOx group as compared to struvite group (G): The color gradient indicates the significance of enrichment. **P* < .05.

Results

Important metabolites and related metabolic pathways in the urine of dogs with calcium oxalate urolithiasis

Multivariate statistical analysis was performed by OPLS-DA to observe the metabolic differences between the CaOx group and the control group. A clear separation between the 2 groups was observed **(Figure 1)**. The permutation test assured the validity of the OPLS-DA model: R2Y was used to assess fitness, and Q2 was used to indicate the prediction ability of the model. In this model, R2Y = 0.993 and Q2 = 0.747 for the positive ion mode, and R2Y = 0.991 and Q2 = 0.552 for the negative ion mode. To further identify highly correlated differential metabolites between 2 groups, setting the standard of a VIP value greater than 1 and *P* value less than .05, a total of 241 significantly differential metabolites were identified between the 2 groups, with 63 metabolites showing upregulation and the rest showing downregulation. Details of the different metabolites are shown **(Supplementary Table 4)**. The metabolites including trigonelline, (+)-nicotine, 4-hydroxy-5-(dihydroxyphenyl)-valeric acid-*O*-sulphate, phenylalanine hydroxyproline, and asymmetric dimethylarginine (ADMA) showed significant downregulation, while metabolites such as (4E)-3-hydroxyhex-4-enoylcarnitine and L-carnitine showed significant upregulation in the CaOx group. Through enrichment analysis of the pathway where the selected differential metabolites were located, we further screened the metabolic pathway and identified the key pathway with the highest correlation with the differential metabolites. In this study, we selected a *P* value less than .05 as the standard for KEGG pathway enrichment. A total of 9 metabolic pathways were enriched; phenylalanine metabolism and nicotinic acid and nicotinamide metabolism may be involved in the occurrence and development process of calcium oxalate.

Important metabolites and related metabolic pathways in the urine of dogs with struvite urolithiasis

The OPLS-DA model was successfully established to observe the metabolic differences between the struvite group and the control group. A clear separation between the 2 groups was observed **(Figure 2)**. R2Y = 0.991 and Q2 = 0.585 for the positive ion mode, and R2Y = 0.982 and Q2 = 0.552 for the negative ion mode indicated that no overfitting was found. To further screen for highly correlated differential metabolites, setting the same standard of a VIP value greater than 1 and *P* value less than .05, a total of 243 significantly differential metabolites were identified between the 2 groups, with 29 metabolites showing upregulation and the rest showing downregulation. The details of the different metabolites are shown **(Supplementary Table 5)**. Metabolites including octa-3,6-dienedioylcarnitine, cysteinylproline, pyocyanin, and (+)-nicotine showed significant downregulation, while metabolites such as 2-methoxyestriol and aspartyl-γ-glutamate showed upregulation in the struvite group. A total of 32 metabolic pathways were enriched by using a *P* value less than .05 as the standard. The glycerophospholipid metabolic pathway, the cGMP-PKG signaling pathway, protein digestion and absorption, and the cAMP signaling pathway may be involved in the occurrence and development process of struvite.

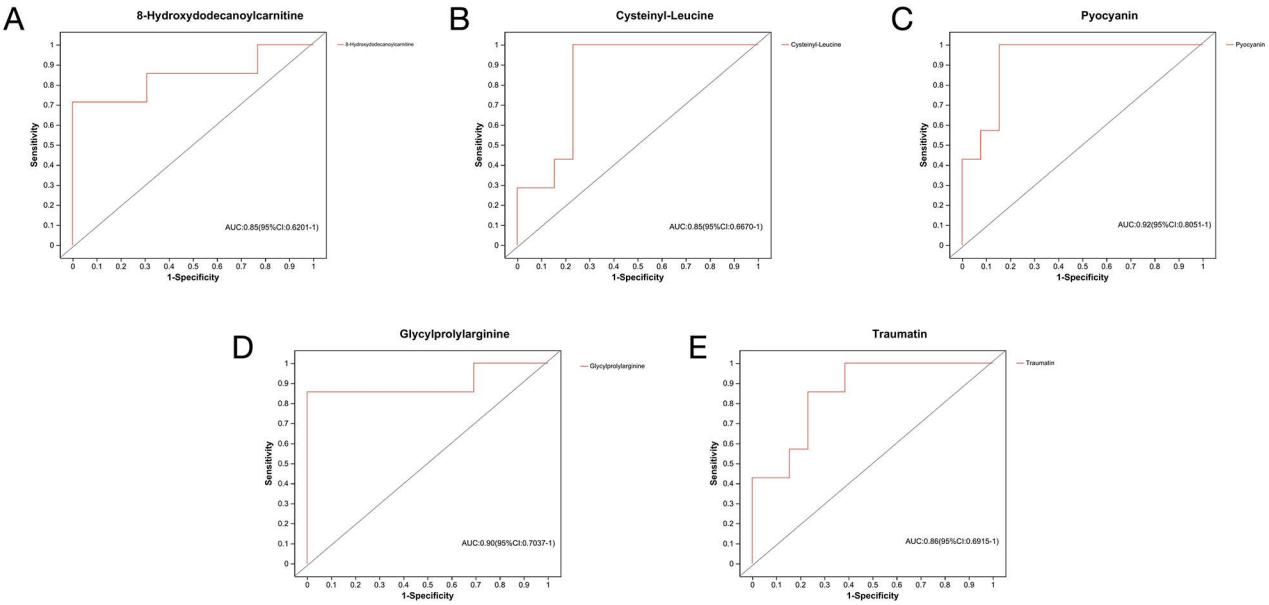

Figure 4—Receiver operating characteristic (ROC; A–E) curve to investigate the diagnostic ability of several candidate biomarkers between the urine of dogs with CaOx (n = 13) and struvite (7) urolithiasis. Area under the ROC curve (AUC) is calculated as percent sensitivity versus 100% specificity. AUC ≥ 0.85 is highly discriminatory.

Candidate urinary biomarkers between the urine of dogs with calcium oxalate and struvite urolithiasis

Between the CaOx group and the struvite group, OPLS-DA was performed to observe the metabolic differences. There was a clear separation between the 2 groups **(Figure 3)**. R2Y = 0.994 and Q2 = 0.395 for the positive ion mode, and R2Y = 0.85 and Q2 = 0.0268 for the negative ion mode indicated that no overfitting was found. Based on the previous OPLS-DA model, setting the standard of a VIP value greater than 1 and *P* value less than .05, a total of 118 significantly differential metabolites were identified between the 2 groups, with 23 metabolites showing downregulation and the rest showing upregulation. Details of the different metabolites are shown **(Supplementary Table 6)**. Metabolites including pyocyanin, tryptophyl-threonine, and prostaglandin B2 showed significant upregulation, while metabolites such as *N*-((2,7-dimethyl-9H-fluoren-9-yl) methoxy) carbonyl)-L-leucine and 9(S)-HpODE showed significant downregulation in the CaOx group. A total of 9 metabolic pathways were enriched by using a *P* value less than .05 as the standard, including the tryptophan metabolism and the arachidonic acid metabolism pathway.

The diagnostic potential of these 118 identified metabolites between the CaOx group and the struvite group was evaluated by the receiver operating characteristic (ROC) curve analysis. The AUC was used to evaluate the reliability of the differential metabolites **(Figure 4)**. The metabolites with AUC values greater than or equal to 0.85, including 8-hydroxydodecylcarnitine (AUC = 0.85), cysteine-leucine (AUC = 0.85), pyocyanin (AUC = 0.92), glycyl prolyl arginine (AUC = 0.90), and traumatin (AUC = 0.86), were among the 20 metabolites.

Discussion

Metabolomic characteristics of urine from dogs with calcium oxalate urolithiasis

The formation of calcium oxalate involves several steps, such as nucleation, crystal growth, aggregation, and retention. Although supersaturated electrolytes in the urine are essential for the formation of calcium oxalate, this is not the only factor contributing to stone formation.[18] The calcium oxalate promoters and inhibitors in the urine also play an important role, so other urinary components besides calcium ions and oxalate remain of interest. Human-related studies[19] have shown that urolithiasis is a systemic disease associated with metabolic syndrome, chronic kidney disease, hypertension, diabetes mellitus, and coronary artery disease. Such systemic diseases affect metabolites throughout the body and are reflected in the urine.

Trigonelline is a biologically active plant compound that can be obtained from the diet or produced as a metabolite derived from nicotinic acid (vitamin B3). Trigonelline has antioxidant and anti-inflammatory activities and plays an important beneficial role in diabetes and Alzheimer disease.[20,21] Previous in vivo studies[22] found that seed extracts of fenugreek, a trigonelline-rich plant, reduced the deposition of calcium oxalate crystals in the kidneys of rats with ethylene glycol-induced renal calculi. It has been shown that trigonelline can prevent kidney stone formation by inhibiting calcium oxalate crystallization, growth, and crystal cell adhesion as well as by downregulating crystal receptors.[23] Meanwhile, a related study[24] performed urine metabolomic analysis in kidney stone patients and found significant downregulation of trigonelline in the kidney stone group. In the present study, trigonelline concentration in the urine of dogs with calcium oxalate was significantly downregulated compared to healthy dogs, which supports that trigonelline can inhibit calcium oxalate stone formation.

(4E)-3-Hydroxyhex-4-enoylcarnitine belongs to the class of organic compounds known as acylcarnitines. More specifically, it is a (4E)-3-hydroxyhex-4-enoic acid ester of carnitine. The general role of acylcarnitine is to transport acyl groups (organic acids and fatty acids) from the cytoplasm to the mitochondria, where they are catabolized to produce energy, a process known as β-oxidation. The kidney plays an important role in carnitine homeostasis in vivo. Under normal physiological conditions, essentially all filtered carnitine is reabsorbed by the renal tubules via an active carnitine transport mechanism. Defective carnitine synthesis has little effect on carnitine stability; in contrast, impaired carnitine transport leads to severe carnitine deficiency, which affects β-oxidation of fatty acids. It is hypothesized that calcium oxalate may cause damage to the epithelial cells of the canine renal tubules, affecting the reabsorption of acylcarnitine and leading to an upregulation of acylcarnitine in the urine of dogs with calcium oxalate urolithiasis.

After enrichment by the KEGG pathway, phenylalanine metabolism and nicotinic acid and nicotinamide metabolism were found to be important pathways associated with calcium oxalate. Metabolites involved in the phenylalanine pathway were significantly downregulated in the urine of dogs with calcium oxalate, with D-cathine and shikimic acid being more pronounced, which is consistent with the results of human urolithiasis studies.[25] Phenylalanine is mostly catabolized through tyrosine, and phenylalanine and its metabolites have been associated with several chronic diseases. Related studies[26] have shown a consistent positive correlation between plasma phenylalanine and the risk of type II diabetes. Phenylalanine is also a precursor substance for catecholamine biosynthesis and can suppress elevated blood pressure by regulating oxygen-free radical scavenging and improving the endocrine function of endothelial cells. The present study speculates that the downregulation of phenylalanine and its related metabolites may suggest a metabolic system disorder, which is associated with concomitant systemic diseases. Nicotinate and nicotinamide metabolic pathways involve niacinamide,

trigonelline, and nicotine. Related to trigonelline mentioned above, renal tubular injury may lead to reduced absorption of niacinamide or nicotinic acid, resulting in the downregulation of related metabolites, suggesting possible renal tubular injury in dogs with calcium oxalate.

This study also focused on L-carnitine and ADMA. L-carnitine was significantly upregulated in the urine of dogs with calcium oxalate urolithiasis compared to healthy dogs. Human studies[8] have found significantly elevated urinary L-carnitine and L-acetylcarnitine in patients with calcium oxalate. Calcium oxalate may cause renal epithelial cell damage, which affects the transport of L-carnitine and L-acetylcarnitine, thereby elevating their levels in the urine.[27] Also, renal epithelial cell injury can affect the interaction between renal tubular epithelial cells and crystals, which is crucial in the development of urolithiasis.[18] This result is consistent with previous observations in a rat calcium oxalate kidney stone model.[4] ADMA is a naturally occurring amino acid derivative involved in the regulation of vascular function and capable of being produced during the breakdown of arginine-containing proteins. ADMA is an endogenous inhibitor of nitric oxide synthase, inhibits nitric oxide synthesis, and is involved in the pathogenesis of many human diseases. The kidney plays a key role in ADMA metabolism, being able to secrete ADMA and expressing high levels of hydrolases to metabolize ADMA. In adults, ADMA has been identified as a biomarker for the chronic kidney disease stage and cardiovascular disease risk and can accelerate the process of kidney injury.[28] The significant downregulation of ADMA in the urine of dogs with calcium oxalate contradicts previous studies[29] suggesting renal injury, and it is speculated that the process of calcium oxalate stone production may increase the expression of ADMA hydrolase, but the exact mechanism needs to be further investigated.

Metabolomic characteristics of urine from dogs with struvite urolithiasis

Urinary metabolomic analysis of the struvite group screened a total of 243 metabolites, of which 29 were upregulated and 214 showed downregulation. Among the differential metabolites, we are mainly interested in pyocyanin, octa-3,6-dienylcarnitine, cysteine proline, 2-methoxyestradiol, and aspartate-γ-glutamate.

The significant differential metabolites of the struvite group were associated with a variety of amino acids. The kidney is an important organ of amino acid metabolism in the animal organism, which can maintain the metabolic balance of amino acids in the body through synthesis, degradation, filtration, reabsorption, and urination; therefore, renal disease can lead to abnormal catabolism of related amino acids (especially of branched-chain amino acids such as leucine, isoleucine, and valine). In the urine of dogs with struvite, leucine derivatives were significantly upregulated, while cysteine proline and aspartate-γ-glutamate were significantly downregulated, and this study suggests that this metabolite profile may be associated with the disturbance of renal amino acid metabolism associated with struvite.

Dogs with struvite are usually accompanied by UTIs associated with urease-producing bacteria, which cause an inflammatory response. Related metabolites in the tryptophan metabolic pathway such as phenylalanine, L-kynurenine, and indoleacrylic acid were downregulated in the struvite group and were considered to be associated with UTIs. Tryptophan is an important essential amino acid for animal organisms, and the main metabolic pathways involved include protein synthesis, the 5-hydroxytryptamine (5-HT) pathway, and the kynurenine pathway. Infection and inflammation can induce and activate some enzymes in the kynurenine pathway, such as indoleamine 2,3-dioxygenase (IDO1).[30] IDO1 is structurally expressed in animal urogenital epithelial cells, while inflammation-activated interferon-γ can significantly upregulate IDO1,[31] so that upregulated IDO1 can accelerate the catabolism of tryptophan-related metabolites, leading to its significant downregulation in dogs with struvite. In contrast, pyocyanin, a pigment released by pathogenic *Pseudomonas aeruginosa* at the site of bacterial infection, can be found in the urinary tract of animals.[32,33] Pyocyanin can assist in respiration, nutrition, and inhibition of competing bacteria by *P aeruginosa*. Pyocyanin was significantly downregulated in the struvite group, presumably because the presence of common urease-producing bacteria (*Staphylococcus* spp and *Enterococcus* spp) competitively inhibited the growth of *P aeruginosa*.

The kidney is an energy-intensive organ that depends on a steady supply of nutrients and reliable energy-producing pathways, in which fatty acid metabolism plays an important role. Dysregulation of lipid oxidation, uptake, and production occurs in renal disease states, and these metabolic dysregulations may further contribute to renal injury. Metabolic analysis showed that the metabolites PA [14:1(9Z)/24:1(15Z)], PE (15:0/20:0), and glycerophosphorylcholine, all related to the glycerophospholipid metabolism pathway, were upregulated in the struvite group. Also, 2-methoxyestratriol was significantly upregulated. It is an in vivo metabolite of estrogen and belongs to the downstream 16β-hydroxylation pathway and 2,4-hydroxylation pathway.[34] 2-Methoxyestriol has been found to have a hypocholesterolemia effect and an impact on lipoprotein metabolism, which could be used to treat hyperlipidemia and atherosclerosis in humans.[35,36] However, the mechanism of action of this hormone in lipid metabolism is not clear.

Candidate urinary biomarker between the urine of dogs with calcium oxalate and struvite urolithiasis

The common types of stones in canine urolithiasis are calcium oxalate and struvite, which are treated differently. At present, the only way to accurately determine stone composition is to remove the stones and perform stone analysis. To reduce surgical

injuries in animals and to advance the precise treatment of canine urolithiasis, urine from dogs with calcium oxalate and struvite urolithiasis was subjected to metabolomic analysis and screened for differential metabolites to explore candidate biomarkers. A total of 118 known metabolites were screened for significant differences between the 2 groups, with 23 metabolites showing downregulation and the rest showing upregulation.

The KEGG pathway was enriched for tryptophan metabolism, and the arachidonic acid metabolism pathway was found to be of interest. 5-Methoxytryptamine is the main metabolite involved in the 5-HT pathway of tryptophan metabolism. 5-HT plays an important role in inflammation and immunity and can regulate various physiological functions. Also, tryptophan metabolites act as ligands to activate signaling in various diseases such as inflammation, oxidative stress injury, cancer, aging-related diseases, cardiovascular disease, and chronic kidney disease.[37] The effect of 5-HT and dopamine on renal Na^+-K^+-ATPase activity was also found in rat renal tubules but was not verified in dogs.[38] The upregulation of metabolites related to the tryptophan-5-HT pathway in the urine of dogs with calcium oxalate, combined with the above findings, leads to the speculation that oxidative stress may be present in the affected dogs, suggesting possible renal damage.

Arachidonic acid is a major component of cell membrane lipids and can be converted into various metabolites that trigger various inflammatory responses, which are thought to be closely related to stone formation. The arachidonic acid metabolism among the differential metabolites in this screening mainly involved prostaglandin B2 and 6-keto-prostaglandin F1α and were significantly elevated in the calcium oxalate group. Prostaglandin B2 is a product of prostaglandin E2 dehydration synthesis, and prostaglandin B2 reduces mean arterial pressure and increases renal blood flow. A study[39] on diabetic nephropathy in rats found that prostaglandin B2 was significantly upregulated in the serum of rats with diabetic nephropathy and that prostaglandin B2 and prostaglandin E2 have similar effects, leading to insulin resistance and accelerated kidney damage. A study[40] in children with urolithiasis found elevated prostaglandin E2 in patients with calcium oxalate, and elevated prostaglandin E2 can further enhance calcium excretion by affecting renal tubular function and the intestine and promote stone formation by inducing oxidative stress-mediated apoptosis of renal tubular epithelial cells. Thus, a positive feedback mechanism may exist between prostaglandin E2 and calcium oxalate stone formation, thus promoting stone occurrence and recurrence.[40] The above findings are consistent with the results in the present study. 6-Keto-prostaglandin F1α is the most direct metabolite of prostate growth factor.[41] Intrarenal prostaglandins are important in regulating renal blood flow, and there are significant changes in urinary prostaglandins in patients with renal vascular hypertension, nephrotic syndrome, and chronic renal failure. Also, 6-keto-prostaglandin F1α has been shown to be a biomarker of oxidative stress, and 6-keto-prostaglandin F1α was significantly elevated in acute kidney injury patients.[42] Combining the above findings, it is hypothesized that dogs with calcium oxalate may have renal inflammation and oxidative stress injury.

In this study, ROC analysis was performed on the characteristic differential metabolites between the calcium oxalate group and struvite group, and metabolites with good sensitivity and specificity were screened by AUC values. The AUC values of 20 metabolites, including pyocyanin (AUC = 0.92), glycyl prolyl arginine (AUC = 0.90), traumatin (AUC = 0.86), cysteine-leucine (AUC = 0.85), and 8-hydroxydodecylcarnitine (AUC = 0.85), were greater than or equal to 0.85, suggesting that these metabolites may have good potential to distinguish different stone. Traumatin is involved in the α-linolenic acid metabolic pathway, and α-linolenic acid is a long-chain n-3 polyunsaturated fatty acid; relevant studies[43,44] have shown that the activity of traumatin is similar to that of unsaturated fatty acids, with antioxidative stress, anti-inflammatory, and procatabolic effects. It is considered to be related to the activation of α-linolenic acid metabolism by UTIs in dogs with struvite. The nontargeted metabolomics analysis of differential metabolites in this study can only explore the candidate biomarkers of the above metabolites, and further targeted verification is needed to verify the candidate biomarker's prediction ability.

The limitation of the study is that, within the group of dogs with struvite urolithiasis, 5 out of 7 were found to have UTIs, highlighting a significant proportion. Therefore, we cannot ascertain whether the candidate urinary biomarker identified can effectively distinguish between sterile struvite urolithiasis and calcium oxalate urolithiasis. Initially, the experiment was designed considering that canine struvite urolithiasis is primarily associated with UTIs. We aimed to investigate the natural variations in the metabolic pathways affected by struvite urolithiasis in dogs to better elucidate the disease mechanism and to explore potential biomarkers for common clinical scenarios of calcium oxalate versus struvite urolithiasis. It is uncertain to what extent UTIs affect the urinary metabolome of the dog with urolithiasis and whether they influence the identified candidate urinary biomarkers. In the future, we intend to conduct a comparative analysis of urinary metabolites in dogs with sterile struvite urolithiasis versus those with UTI-associated struvite urolithiasis. Additionally, we plan to further explore the effectiveness of the candidate biomarkers in distinguishing between dogs with sterile struvite and calcium oxalate urolithiasis, as well as their effectiveness in differentiating dogs with UTI-associated struvite urolithiasis from those with calcium oxalate urolithiasis.

In conclusion, this study completed the metabolomic analysis of urine samples from dogs with calcium oxalate and struvite urolithiasis and screened a series of differential metabolites, which provided more ideas to elucidate the pathological mechanisms

of different types of stones and filled a gap in relevant small animal clinical studies. This study identified candidate biomarkers in the urine of dogs with struvite and calcium oxalate urolithiasis, which can be further validated for clinical applications and aid in the precise treatment of canine urolithiasis.

Acknowledgments

None reported.

Disclosures

The authors have nothing to disclose. No AI-assisted technologies were used in the generation of this manuscript.

Funding

The research is supported by "The Talent Fund of China Agricultural University Veterinary Teaching Hospital."

References

1. Bartges JW, Callens AJ. Urolithiasis. *Vet Clin North Am Small Anim Pract.* 2015;45(4):747–768. doi:10.1016/j.cvsm.2015.03.001
2. Kopecny L, Palm CA, Segev G, Westropp JL. Urolithiasis in dogs: evaluation of trends in urolith composition and risk factors (2006–2018). *J Vet Intern Med.* 2021;35(3):1406–1415. doi:10.1111/jvim.16114
3. Wagner CA. Etiopathogenic factors of urolithiasis. *Arch Esp Urol.* 2021;74(1):16–23.
4. Gao S, Yang R, Peng Z, et al. Metabolomics analysis for hydroxy-L-proline-induced calcium oxalate nephrolithiasis in rats based on ultra-high performance liquid chromatography quadrupole time-of-flight mass spectrometry. *Sci Rep.* 2016;6:30142. doi:10.1038/srep30142
5. Wen H, Lee T, You S, et al. Urinary metabolite profiling combined with computational analysis predicts interstitial cystitis-associated candidate biomarkers. *J Proteome Res.* 2015;14(1):541–548. doi:10.1021/pr5007729
6. Nizioł J, Ossoliński K, Płaza-Altamer A, et al. Untargeted urinary metabolomics for bladder cancer biomarker screening with ultrahigh-resolution mass spectrometry. *Sci Rep.* 2023;13(1):9802.
7. Zhang X-Z, Lei X-X, Jiang Y-L, et al. Application of metabolomics in urolithiasis: the discovery and usage of succinate. *Signal Transduct Target Ther.* 2023;8(1):41. doi:10.1038/s41392-023-01311-z
8. Wang X, Wang M, Ruan J, Zhao S, Xiao J, Tian Y. Identification of urine biomarkers for calcium-oxalate urolithiasis in adults based on UPLC-Q-TOF/MS. *J Chromatogr B Analyt Technol Biomed Life Sci.* 2019;1124:290–297. doi:10.1016/j.jchromb.2019.06.022
9. Lulich JP, Berent AC, Adams LG, Westropp JL, Bartges JW, Osborne CA. ACVIM small animal consensus recommendations on the treatment and prevention of uroliths in dogs and cats. *J Vet Intern Med.* 2016;30(5):1564–1574.
10. Progenesis QI. Package insert. Waters Corporation. Accessed January 29, 2023. https://www.nonlinear.com/progenesis/qi/
11. Wishart DS, Guo A, Oler E, et al. HMDB 5.0: the human metabolome database. *Nucleic Acids Res.* 2022;50(D1):D622–D631.
12. Montenegro-Burke JR, Guijas C, Siuzdak, G. METLIN: a tandem mass spectral library of standards. *Methods Mol Biol.* 2020;2104:149–163.
13. Ren Y. Majorbio Cloud: a one-stop, comprehensive bioinformatic platform for multi-omics analyses. Majorbio.com. Accessed January 28, 2023. https://cloud.majorbio.com
14. Warrack BM, Hnatyshyn S, Ott KH, et al. Normalization strategies for metabonomic analysis of urine samples. *J Chromatogr B Analyt Technol Biomed Life Sci.* 2009;877(5–6):547–552.
15. Virtanen V, Gommers R, Oliphant TE, et al. SciPy 1.0: fundamental algorithms for scientific computing in Python. *Nat Methods.* 2020;17(3):352. doi:10.1038/s41592-020-0772-5
16. Thevenot EA. PCA, PLS(-DA) and OPLS(-DA) for multivariate analysis and feature selection of omics data. Version 1.6.2. Bioconductor. Accessed January 29, 2023. https://bioconductor.riken.jp/packages/3.4/bioc/manuals/ropls/man/ropls.pdf
17. KEGG: Kyoto Encyclopedia of Genes and Genomes. GenomeNet. Accessed January 28, 2023. https://www.genome.jp/kegg/
18. Aggarwal KP, Narula S, Kakkar M, Tandon C. Nephrolithiasis: molecular mechanism of renal stone formation and the critical role played by modulators. *Biomed Res Int.* 2013;2013:292953. doi:10.1155/2013/292953
19. Sakhaee K, Maalouf NM, Sinnott B. Clinical review. Kidney stones 2012: pathogenesis, diagnosis, and management. *J Clin Endocrinol Metab.* 2012;97(6):1847–1860. doi:10.1210/jc.2011-3492
20. Costa MC, Lima TFO, Arcaro CA, et al. Trigonelline and curcumin alone, but not in combination, counteract oxidative stress and inflammation and increase glycation product detoxification in the liver and kidney of mice with high-fat diet-induced obesity. *J Nutr Biochem.* 2020;76:108303. doi:10.1016/j.jnutbio.2019.108303
21. Farid MM, Yang X, Kuboyama T, Tohda C. Trigonelline recovers memory function in Alzheimer's disease model mice: evidence of brain penetration and target molecule. *Sci Rep.* 2020;10(1):16424. doi:10.1038/s41598-020-73514-1
22. Laroubi A, Touhami M, Farouk L, et al. Prophylaxis effect of Trigonella foenum graecum L. seeds on renal stone formation in rats. *Phytother Res.* 2007;21(10):921–925. doi:10.1002/ptr.2190
23. Peerapen P, Boonmark W, Thongboonkerd V. Trigonelline prevents kidney stone formation processes by inhibiting calcium oxalate crystallization, growth and crystal-cell adhesion, and downregulating crystal receptors. *Biomed Pharmacother.* 2022;149:112876. doi:10.1016/j.biopha.2022.112876
24. Thongprayoon C, Vuckovic I, Vaughan LE, et al. Nuclear magnetic resonance metabolomic profiling and urine chemistries in incident kidney stone formers compared with controls. *J Am Soc Nephrol.* 2022;33(11):2071–2086. doi:10.1681/ASN.2022040416
25. Atanassova SS, Panchev P, Ivanova M. Plasma levels and urinary excretion of amino acids by subjects with renal calculi. *Amino Acids.* 2010;38(5):1277–1282. doi:10.1007/s00726-009-0359-z
26. Zou B, Sun Y, Xu Z, et al. Rapid simultaneous determination of gut microbial phenylalanine, tyrosine, and tryptophan metabolites in rat serum, urine, and faeces using LC-MS/MS and its application to a type 2 diabetes mellitus study. *Biomed Chromatogr.* 2021;35(2):e4985. [10.1002/bmc.4985]
27. El-Hattab AW, Scaglia F. Disorders of carnitine biosynthesis and transport. *Mol Genet Metab.* 2015;116(3):107–112. doi:10.1016/j.ymgme.2015.09.004
28. Tripepi G, Mattace Raso F, Sijbrands E, et al. Inflammation and asymmetric dimethylarginine for predicting death and cardiovascular events in ESRD patients. *Clin J Am Soc Nephrol.* 2011;6(7):1714–1721. doi:10.2215/CJN.11291210
29. Jacobi J, Tsao PS. Asymmetrical dimethylarginine in renal disease: limits of variation or variation limits? A systematic review. *Am J Nephrol.* 2008;28(2):224–237. doi:10.1159/000110092

30. Klaessens S, Stroobant V, De Plaen E, Van den Eynde BJ. Systemic tryptophan homeostasis. *Front Mol Biosci.* 2022;9:897929. doi:10.3389/fmolb.2022.897929
31. Theate I, van Baren N, Pilotte L, et al. Extensive profiling of the expression of the indoleamine 2,3-dioxygenase 1 protein in normal and tumoral human tissues. *Cancer Immunol Res.* 2015;3(2):161–172. doi:10.1158/2326-6066.CIR-14-0137
32. Mossine VV, Waters JK, Chance DL, Mawhinney TP. Transient proteotoxicity of bacterial virulence factor pyocyanin in renal tubular epithelial cells induces ER-related vacuolation and can be efficiently modulated by iron chelators. *Toxicol Sci.* 2016;154(2):403–415. doi:10.1093/toxsci/kfw174
33. Hall JL, Holmes MA, Baines SJ. Prevalence and antimicrobial resistance of canine urinary tract pathogens. *Vet Rec.* 2013;173(22):549. doi:10.1136/vr.101482
34. Takahashi M, Shimomoto T, Miyajima K, et al. Effects of estrogens and metabolites on endometrial carcinogenesis in young adult mice initiated with N-ethyl-N'-nitro-N-nitrosoguanidine. *Cancer Lett.* 2004;211(1):1–9. doi:10.1016/j.canlet.2004.01.029
35. Kono S, Matsumura M, Higa H, Sunagawa H. [Hypocholesterolemic effect of catechol estrogen 2-monomethyl ether]. *Nihon Naibunpi Gakkai Zasshi.* 1987;63(5):712–717.
36. Higa H. [Effects of catecholestrogen and catecholestrogen 2-monomethyl ether on serum lipids and lipoproteins in rats]. *Igaku Kenkyu.* 1990;60(1):1–17.
37. Liu JR, Miao H, Deng DQ, Vaziri ND, Li P, Zhao YY. Gut microbiota-derived tryptophan metabolism mediates renal fibrosis by aryl hydrocarbon receptor signaling activation. *Cell Mol Life Sci.* 2021;78(3):909–922. doi:10.1007/s00018-020-03645-1
38. Soares-da-Silva P, Cabral JM, Magalhaes D, Fraga S, Magro F. Amine neurotransmitters, inflammation and epithelial sodium transport. *Exp Physiol.* 2016;101(4):459–464. doi:10.1113/EP085284
39. Zhang B, Wan Y, Zhou X, et al. Characteristics of serum metabolites and gut microbiota in diabetic kidney disease. *Front Pharmacol.* 2022;13:872988. doi:10.3389/fphar.2022.872988
40. Wen J, Cao Y, Li Y, et al. Metabolomics analysis of the serum from children with urolithiasis using UPLC-MS. *Clin Transl Sci.* 2021;14(4):1327–1337. doi:10.1111/cts.12984
41. Chappell DL, Xiao X, Radziszewski W, Laterza OF. Development and validation of a LC/MS/MS method for 6-keto PGF1alpha, a metabolite of prostacyclin (PGI(2)). *J Pharm Biomed Anal.* 2011;56(3):600–603. doi:10.1016/j.jpba.2011.06.019
42. Radovanovic S, Savic-Radojevic A, Pljesa-Ercegovac M, et al. Markers of oxidative damage and antioxidant enzyme activities as predictors of morbidity and mortality in patients with chronic heart failure. *J Card Fail.* 2012;18(6):493–501. doi:10.1016/j.cardfail.2012.04.003
43. Jablonska-Trypuc A, Pankiewicz W, Czerpak R. Traumatic acid reduces oxidative stress and enhances collagen biosynthesis in cultured human skin fibroblasts. *Lipids.* 2016;51(9):1021–1035. doi:10.1007/s11745-016-4174-5
44. Cambiaggi L, Chakravarty A, Noureddine N, Hersberger M. The role of alpha-linolenic acid and its oxylipins in human cardiovascular diseases. *Int J Mol Sci.* 2023;24(7):6110.

Supplementary Materials

Supplementary materials are posted online at the journal website: avmajournals.avma.org